Isolating a violet stimulated luminescence (VSL) signal in quartz suitable for dating

Ataee, Nina; Roberts, Helen M.; Duller, Geoff A.t.

Published in:
Radiation Measurements

DOI:
10.1016/j.radmeas.2022.106810

Publication date:
2022

Citation for published version (APA):
Ataee, N., Roberts, H. M., & Duller, G. A. T. (2022). Isolating a violet stimulated luminescence (VSL) signal in quartz suitable for dating: Investigating different thermal treatments and signal integration limits. *Radiation Measurements*, *156*, [106810]. https://doi.org/10.1016/j.radmeas.2022.106810

Radiation Measurements 156 (2022) 106810

Contents lists available at ScienceDirect

Radiation Measurements

journal homepage: www.elsevier.com/locate/radmeas

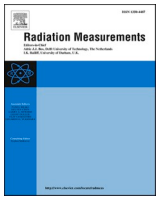

Isolating a violet stimulated luminescence (VSL) signal in quartz suitable for dating: Investigating different thermal treatments and signal integration limits

Nina Ataee *, Helen M. Roberts, Geoff A.T. Duller

Department of Geography and Earth Sciences, Aberystwyth University, Aberystwyth, SY23 3DB, Wales, United Kingdom

ARTICLE INFO

Keywords:
VSL
Dose recovery
Equivalent dose
D_e
Signal integration limits
Preheat

ABSTRACT

The behavior of the post-blue violet stimulated luminescence (VSL) signal from quartz with respect to thermal treatments is explored. The results suggest that more than one source trap may be responsible for the VSL signal and therefore, the separation of this signal from the preceding blue stimulated luminescence (BSL) signal is challenging. Furthermore, the behavior of the VSL dose response curve (DRC) in a single aliquot regenerative (SAR) protocol is demonstrated to be influenced significantly by the test dose size and the efficacy of signal depletion prior to measurement of the test dose signal, and hence a modified VSL SAR measurement protocol is considered for further investigations in this study. The ability of this protocol to recover a given dose is tested and it is shown that by selecting different integration limits, two signals with distinct dose response characteristics can be separated from the same original VSL decay curve. Dose response curves derived from early signal integration (Signal A) saturate at ~150 Gy and cannot recover given doses beyond this limit, whereas later signal integration (Signal B) results in a DRC that continues to grow exponentially to doses >> 500 Gy, and can recover given doses up to at least ~3200 Gy. However, Signal B underestimates by ~90% the equivalent dose (D_e) for a sample with expected D_e value of ~500 Gy. This may suggest thermal instability of Signal B over geological time and needs further investigation.

1. Introduction

Violet stimulated luminescence (VSL) is a relatively new technique in optically stimulated luminescence (OSL) research that utilizes violet light (~405 nm) to optically stimulate quartz grains, reaching deeper traps not accessible by blue light (Jain, 2009). The main reason for using the VSL signal instead of the conventional quartz OSL signal stimulated with blue (~470 nm) light (blue stimulated luminescence; BSL) is because the VSL signal is thought to grow to higher doses and hence would be able to date older sediments. However, from recent research it seems that the VSL signal generally fails to extend the dose range beyond the limits of conventional quartz BSL (Ankjærgaard et al., 2013, 2015, 2016; Morthekai et al., 2015; Colarossi et al., 2018a; Porat et al., 2018; Sontag-González et al., 2021; Rahimzadeh et al., 2021). The origins and behavior of the VSL signal have been investigated previously (Jain, 2009; Ankjærgaard et al., 2013, 2015; Hernandez and Mercier, 2015); however, ambiguity about the traps (or recombination centers) giving rise to this signal has resulted in the use of a wide range of thermal treatments in VSL protocols, for both single aliquot and multiple aliquot methods (Table 1). Currently, there is no consensus on the most appropriate measurement protocols and/or thermal treatments for use in VSL dating.

The aim of this study is to improve our understanding of the VSL signal. Different characteristics of this signal are explored in this paper: first, the response to thermal treatments is investigated to study the relationship between the BSL (measured prior to the VSL) and VSL signals, and thus select a preheat to isolate a VSL signal distinct from the BSL. Secondly, the dose response behavior is examined with respect to the test dose size and resetting of the VSL signal within a single aliquot regenerative (SAR) dose sequence. This helps to refine a VSL SAR protocol for dating. Thirdly, to test the suitability of the new VSL SAR protocol, the ability to recover different laboratory-given doses is explored. Finally, VSL is used to determine the equivalent dose (D_e) for three samples from a site in Zambia with different expected D_e values.

* Corresponding author.
E-mail address: nia12@aber.ac.uk (N. Ataee).

https://doi.org/10.1016/j.radmeas.2022.106810
Received 23 December 2021; Received in revised form 13 May 2022; Accepted 3 June 2022
Available online 9 June 2022

2. Samples and instrumentation

2.1. Samples

The samples used in this study are sediments from the archeological site of Kalambo Falls in northern Zambia (Duller et al., 2015). This site is of great archeological importance since it sheds light on the timing of Stone Age technological changes in south-central Africa (Barham et al., 2015). Three samples (Aber105/KB1, KB7, KB9) were selected from two of the excavation units (C2 and C3) (see Barham et al., 2015 and Duller et al., 2015 for detailed site description). The age of these samples has been determined previously by single grain quartz BSL for the youngest two samples (KB1: 0.49 ± 0.02 ka and KB9: 43.7 ± 2.0 ka) and by multiple grain thermally-transferred OSL (TT-OSL) for the oldest sample (KB7: 339 ± 49 ka) (Duller et al., 2015). The oldest sample (KB7) was included in this study since the region beyond ~150 Gy is where the BSL signal typically saturates and a particular area of interest is to see whether the dose range of quartz can be extended using the VSL signal. In the present study, coarse grain quartz (180–212 μm) was mounted on steel cups (3 mm diameter aliquots) using Silkospray™ silicone oil. Sample KB1 was used to a) investigate the thermal treatment behavior (section 3), b) refine the VSL SAR protocol (section 4), and c) study the dose response behavior while recovering various doses (section 5). In a) and b) an annealed aliquot of sample KB1 was used, while fresh aliquots of this sample were used in c). All three samples from Kalambo Falls had their D_e measured using the newly developed VSL protocol (discussed in section 6).

2.2. Instrumentation and measurement parameters

All luminescence measurements were performed on an automated Risø TL/OSL DA-20 reader equipped with a DASH head (Lapp et al., 2015), with blue LEDs (470 nm; full power 88 mW cm^{-2}) and a violet laser diode (405 nm; full power 50 mW cm^{-2}) for optical stimulation. All VSL measurements used the violet laser diode at full power, and unless otherwise stated the blue LEDs were operated at 17.6 mW cm^{-2} to avoid the BSL signal being too bright for the photomultiplier tube. Both blue stimulated luminescence (BSL) and violet stimulated luminescence (VSL) signals were detected with an Electron Tubes EMD-9107 photomultiplier tube equipped with a combination of a Semrock Brightline 340 nm (FF01-340/26) filter and 5 mm of Hoya U340 filter. Samples were irradiated by a ^{90}Sr/^{90}Y beta source delivering a dose rate of ~0.077 Gy s^{-1} to coarse grain quartz on steel cups. For dose recovery and residual measurements aliquots were bleached in a Hönle SOL2 solar simulator for 24 h. A fixed measurement temperature of 125 °C was used for both BSL and VSL to avoid retrapping of charge in the 110 °C TL peak (Murray and Wintle, 2000) except for the thermal quenching experiment discussed in section 3.3. All VSL readings for signal measurement (as distinct from signal reduction between measurement steps) were recorded for a duration of ~1000 s (delivering ~50 J cm^{-2} to the sample). In sections 3 and 4, signal and background integration limits are the first 4 s and last 16 s respectively for the VSL signal. In section 3, the first 1.2 s for the signal and last 4 s for the background are integrated for the BSL signal. The recycling ratio is within uncertainties of unity for all the reported results in sections 5 and 6.

3. Exploring the behavior of the VSL signal in response to thermal treatments

To explore the impact of thermal treatment in the VSL SAR sequence used for dose measurement, three different experiments were performed, namely: a) pulse annealing, b) TL signal loss after BSL and VSL stimulations, and c) dependence of the VSL (and BSL) signals upon measurement temperature. These experiments were conducted on a single aliquot of sample KB1 that had been annealed to 450 °C several times to remove any existing natural signal prior to the start of these measurements, and to condition the sample to minimize sensitivity change in subsequent steps.

Table 1
Sequences used previously to measure the VSL signal. In the sixth column, Faershtein et al. (2020) used the same sequence as Ankjærgaard et al. (2015) but applied MAAD (multiple aliquot additive dose). In the seventh column, Ankjærgaard et al. (2016) used their sequence to assess both SAR and MAAD protocols; however, Sontag-González et al. (2021) used this sequence only for MAAD and modified it further by reducing the duration of the preheat to 10 s. MAR in the last two columns refer to multiple aliquot regenerative dose.

SAR					SAR MAAD		SAR MAR	MAAD MAR
Jain (2009)	Ankjærgaard et al. (2013); Morthekai et al. (2015)	Hernandez and Mercier (2015); Sontag-González et al. (2021)	Colarossi et al. (2018a)	Ankjærgaard (2019)	Ankjærgaard et al. (2015); Faershtein et al. (2020)	Ankjærgaard et al. (2016); Sontag-González et al. (2021)	Rahimzadeh et al. (2021)	Ankjærgaard (2019)
Preheat (340 °C, 10s)		Preheat (260 °C, 10s)	Preheat (280 °C, 10s)	Preheat (300 °C, 100s)	Preheat (300 °C, 100s)	Preheat (300 °C, 100s)	Preheat (280 °C, 10s)	Preheat (300 °C, 100s)
BSL (125 °C, 100s)	BSL (280 °C, 100s)	BSL (125 °C, 40s)	BSL (125 °C, 40s)	BSL (125 °C, 100s)	BSL (125 °C, 100s)	BSL (125 °C, 100s)	BSL (125 °C, 40s)	BSL (125 °C, 100s)
VSL (20 °C, 500s)	VSL (125 °C, 100s)	VSL (? 500s)	VSL (30 °C, 500s)	VSL (30 °C, 500s)	VSL (30 °C, 500s)	VSL (30 °C, 500s)	VSL (125 °C, 500s)	VSL (30 °C, 500s)
		VSL (200 °C, 500s)	VSL (200 °C, 500s)				VSL (240 °C, 500s)	
Test dose	Test dose	Test dose	Test dose	Test dose	Test dose	Test dose	Test dose	Test dose
Preheat (340 °C, 1s)		Preheat (260 °C, 10s)	Preheat (280 °C, 10s)	Preheat (300 °C, 100s)	Preheat (290 °C, 100s)	Preheat (300 °C, 100s)	Preheat (280 °C, 10s)	Preheat (300 °C, 100s)
BSL (125 °C, 100s)	BSL (270 °C, 100s)	BSL (125 °C, 40s)	BSL (125 °C, 40s)	BSL (125 °C, 100s)	BSL (125 °C, 100s)	BSL (125 °C, 100s)	BSL (125 °C, 40s)	BSL (125 °C, 100s)
VSL (20 °C, 500s)	VSL (125 °C, 100s)	VSL (? 500s)	VSL (30 °C, 500s)	VSL (30 °C, 500s)	VSL (30 °C, 500s)	VSL (30 °C, 500s)	VSL (125 °C, 500s)	VSL (30 °C, 500s)
BSL (500 °C, 100s)	VSL (280 °C, 200s)	VSL (200 °C, 500s)	VSL (200 °C, 500s)	VSL (280 °C, 200s)	VSL (380 °C, 200s)	TL (500 °C, 20s)	VSL (240 °C, 500s)	

3.1. Pulse annealing

To explore the effect of different preheat temperatures upon the BSL and VSL signals, and potentially help select the appropriate preheat temperature(s) for VSL SAR measurement protocols, a pulse annealing experiment was performed on sample KB1 as described in Table 2a. The sample was given a dose of ~62 Gy and preheated to temperatures from between 200 and 380 °C in 20 °C increments before having its BSL and then VSL signals measured. A test dose of ~39 Gy was used to monitor for sensitivity change, with a preheat of 280 °C for all test doses. Two repeat points at preheats of 200 and 300 °C were measured after the highest preheat (380 °C) and as shown in Fig. 1c, the repeat points overlap with the first measurements demonstrating that the sensitivity correction was appropriate. Fig. 1a and b shows a series of BSL and VSL decay curves after different preheats. At high preheat temperatures the BSL signal becomes very low, with the signal at the end of the 100 s stimulation being close to the photomultiplier dark count (Fig. 1a). The VSL signal also decreases in intensity with increasing preheat, but regardless of preheat it is interesting to note that there is still a substantial signal (~2000 counts per 4 s after ~1000 s of stimulation) observed at the end of the VSL decay curve (Fig. 1b). The relatively high signal observed at the end of all these VSL measurements may be due to breakthrough, as observed previously by Lapp et al. (2012). The use of one thousand seconds of violet stimulation is much longer than used in previous studies (Table 1), but this extended duration measurement to deplete the VSL signal is important when applying regenerative dose methods that inherently rely upon resetting the signal of interest during each cycle.

The first part of the VSL and BSL signals, both with late background subtraction were used for the analysis of signal loss due to preheat temperature. Fig. 1c shows the reduction of the normalized (L_x/T_x) BSL and VSL signals as preheat temperature is increased. The BSL signal remains consistent for preheats from 200 to ~260 °C, similar to many previous observations of the fast component of the BSL signal (e.g. Singarayer and Bailey, 2003; Roberts and Duller, 2004), and then drops rapidly above 280 °C until reaching very low levels at 340 °C and higher. This pattern is thought to reflect the dominant contribution from the 325 °C TL peak, and its thermal erosion at preheats of 280 °C and above (Roberts and Duller, 2004). In contrast, the VSL signal remaining after measurement of the BSL signal shows a monotonic decrease at all temperatures from 200 to 340 °C. This difference between BSL and VSL signals is almost identical to that observed by Jain (2009) and implies that VSL can be obtained from a range of traps in quartz. The decrease in VSL signal seen in Fig. 1c is similar to that seen for the BSL slow components named S2 in Singarayer and Bailey (2003) and S3 in Jain et al. (2003), suggesting the same traps responsible for the BSL slow components may contribute charge to the VSL signal. One of the aims of a thermal pretreatment for VSL measurements is to isolate a VSL signal distinct from the fast component BSL signal. In Fig. 1c the VSL/BSL ratio is largest for a preheat of 340 °C (see the inset), minimizing the potential contribution of the source trap of the fast component BSL signal to the

Table 2
The sequences used in the a) pulse annealing, b) loss of TL, and c) thermal quenching experiments. For a) Step 2, T starts from 200 °C and increases in 20 °C increments up to 380 °C. c) Steps 3 and 4, BSL and VSL measurement temperature were increased from 25 to 300 °C in 25 °C increments.

	a) Pulse annealing	b) Loss of TL	c) Thermal quenching
Step	Treatment		
1	Dose ~62 Gy	Dose ~383 Gy	Dose ~62 Gy
2	Preheat at T °C for 10 s	Preheat to 340 °C for 10 s	Preheat to 340 °C for 10 s
3	BSL at 125 °C for 100 s	BSL at 125 °C for 100 s	BSL at T °C for 100 s
4	VSL at 125 °C for 1000 s	TL to 550 °C and hold for 10 s	VSL at T °C for 1000 s
5	Test dose ~39 Gy	VSL at 310 °C for 200 s	Test dose ~39 Gy
6	Preheat to 280 °C for 10 s	Dose ~383 Gy	Preheat to 340 °C for 10 s
7	BSL at 125 °C for 100 s	Preheat to 340 °C for 10 s	BSL at 125 °C for 100 s
8	VSL at 125 °C for 1000 s	BSL at 125 °C for 100 s	VSL at 125 °C for 1000 s
9	VSL at 380 °C for 200 s	VSL at 125 °C for 1000 s	VSL at 380 °C for 200 s
10		TL to 550 °C and hold for 10 s	
11		VSL at 310 °C for 200 s	

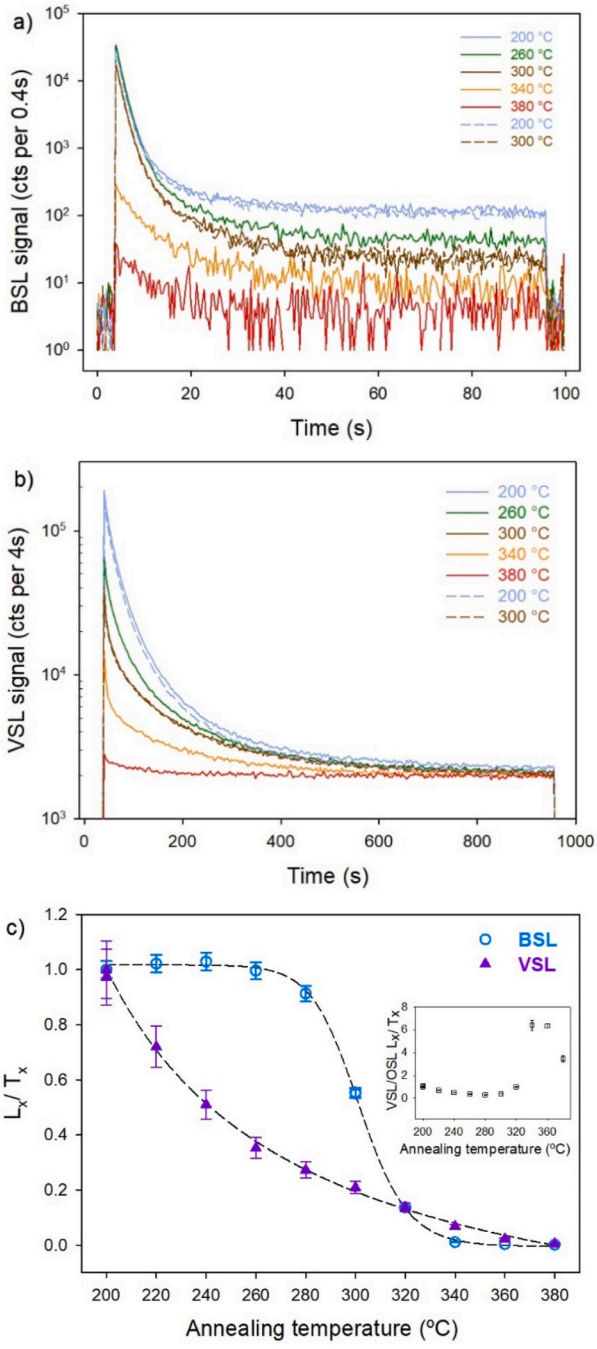

Fig. 1. a) BSL decay curves after various preheats in the pulse annealing experiment. b) Same as a) for VSL decay curves. c) Reduction of the L_x/T_x signals with preheat temperature in the pulse annealing experiment. L_x/T_x values are normalized to the first measurement point. Inset shows the VSL/BSL ratio of the L_x/T_x signals. Measurement was performed on an annealed aliquot of sample KB1.

following VSL signal. In subsequent experiments this preheat temperature of 340 °C was used.

3.2. Origin of the VSL signal: information from thermoluminescence

A considerable portion of the VSL signal is thought to originate from the trap associated with the ~375 °C TL peak (Ankjærgaard et al., 2013; Hernandez and Mercier, 2015). To test whether this is the case for sample 105/KB1, the loss of TL due to the VSL measurement was investigated using the sequence outlined in Table 2b. The TL curve to 550 °C (heating rate 2 °C/s) was recorded after measuring the BSL signal only (blue LED power 62 mW cm^{-2}), then the cycle was repeated to measure the TL signal following BSL and (post-BSL) VSL stimulations. These measurements were repeated three times and minimal sensitivity change was observed; the relative standard deviation between these three replicate measurements is 5% for the TL recorded after BSL and 4% for the TL recorded after BSL plus VSL. Fig. 2a shows the TL data obtained following these BSL and VSL measurements. Fig. 2b shows the difference between the TL peaks (the TL loss) after these two optical stimulations, indicating a clear loss of TL signal in the 350–390 °C TL region, consistent with the primary source being a TL peak at ~375 °C. Fig. 2c shows the ratio of the TL curves revealing that ~80% of the signal is lost after VSL stimulation and there is some signal loss, although to a smaller degree, at both higher and lower temperatures (from 250 to 450 °C).

3.3. Origin of the VSL signal: exploring the impact of measurement temperature

The previous experiment (section 3.2) confirmed the suggestion made by previous research that much of the VSL signal is associated with charge that contributes to the TL peak at 375 °C. This attribution raises some interesting issues based on earlier research into the nature of this TL peak. The 375 °C TL peak is part of what Franklin et al. (1995) termed the 'slowly bleaching family' of traps associated with emission at ~470 nm, and does not appear to be affected by thermal quenching (Franklin et al., 1995). In contrast, the 325 °C TL peak (part of a second group of peaks, the 'rapidly bleaching family' of Franklin et al., 1995) is associated with the fast BSL component emitting at wavelengths below 430 nm and is strongly affected by thermal quenching (Wintle, 1975). So how does the VSL signal, detected at wavelengths of ~340 nm (FWHM 26 nm), vary with measurement temperature?

The sequence outlined in Table 2c was applied to the same annealed aliquot of sample KB1. A fixed preheat (340 °C) was used, and BSL and VSL measurement temperatures were increased from 25 to 300 °C in 25 °C increments. The lowest measurement temperature (25 °C) was repeated at the end of the cycle of increasing measurement temperatures, and the measured L_x/T_x values for the two measurements at 25 °C were within 2σ, demonstrating that any sensitivity change was accounted for. Fig. 3a and b shows a series of BSL and VSL decay curves with different measurement temperatures. The first part of the VSL and BSL signals both with late background subtraction was used. As illustrated in Fig. 3c, quenching becomes dominant between ~150 °C and 250 °C for both signals. Below ~150 °C both signals increase; however, this is more pronounced for the VSL signal. This process is similar to the previously observed phenomenon of thermal assistance for the BSL signal, where eviction of electrons from the source traps by photon absorption (photoeviction) can be enhanced thermally (Spooner, 1994). Above ~250 °C the VSL signal appears to increase. It is notable that the VSL signal measured at the end of the 1000 s of violet stimulation differs by almost 2 orders of magnitude across the range of measurement temperatures (Fig. 3b and d), whilst the BSL shows limited change (Fig. 3a). It was previously concluded that the signal remaining at the end of the VSL measurement was the result of breakthrough (section 3.1, Lapp et al., 2012), but breakthrough would not be expected to change with measurement temperature. To explore this further, the sequence in

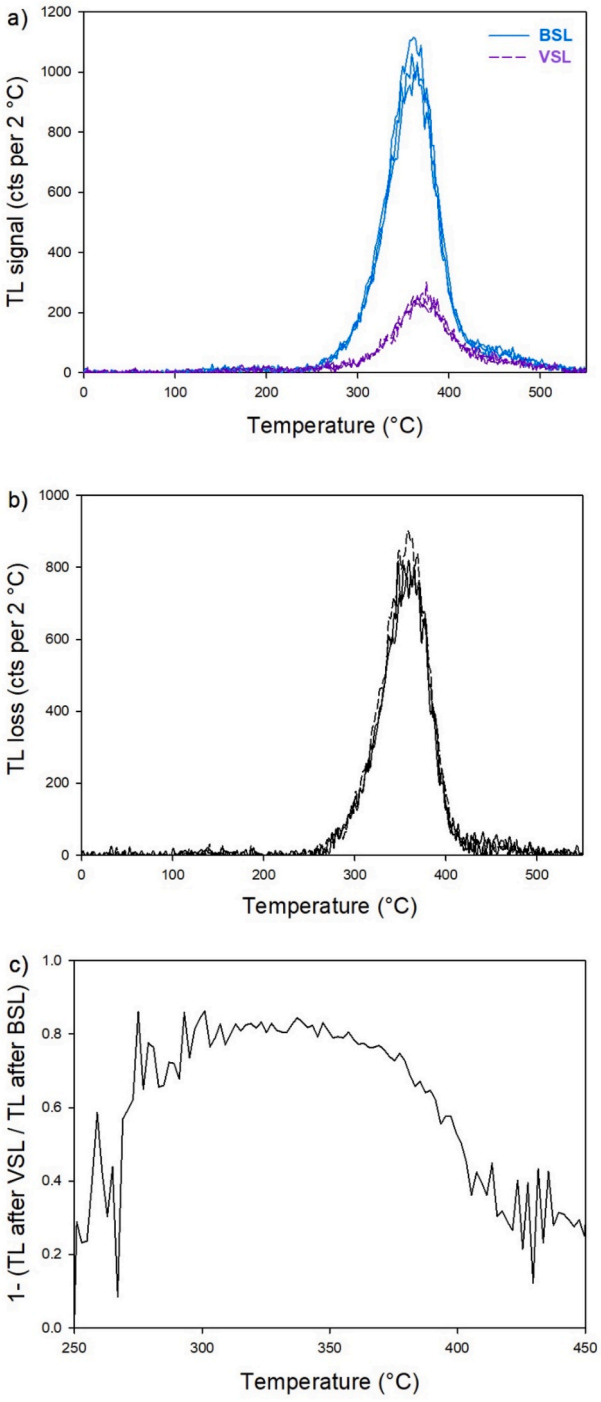

Fig. 2. a) TL curves for an annealed aliquot of KB1 recorded after BSL-only and after blue plus violet stimulation (post-BSL VSL), using the sequence outlined in Table 2b b) TL loss calculated as the difference between the TL curves obtained following BSL-only and post-BSL VSL measurements. c) The ratio of the two sets of TL curves. The three curves were averaged.

Table 2c was repeated for two empty steel cups. A high signal was observed when the violet stimulation was switched on and, as one would expect, this did not vary with stimulation time. However, the absolute magnitude of this constant signal increased consistently as the measurement temperature increased (Fig. 3d). This is not consistent with simple breakthrough of the violet stimulation through the detection filters, and we do not currently understand what process is responsible for this increase. Fig. 3d shows that although the signal from the empty

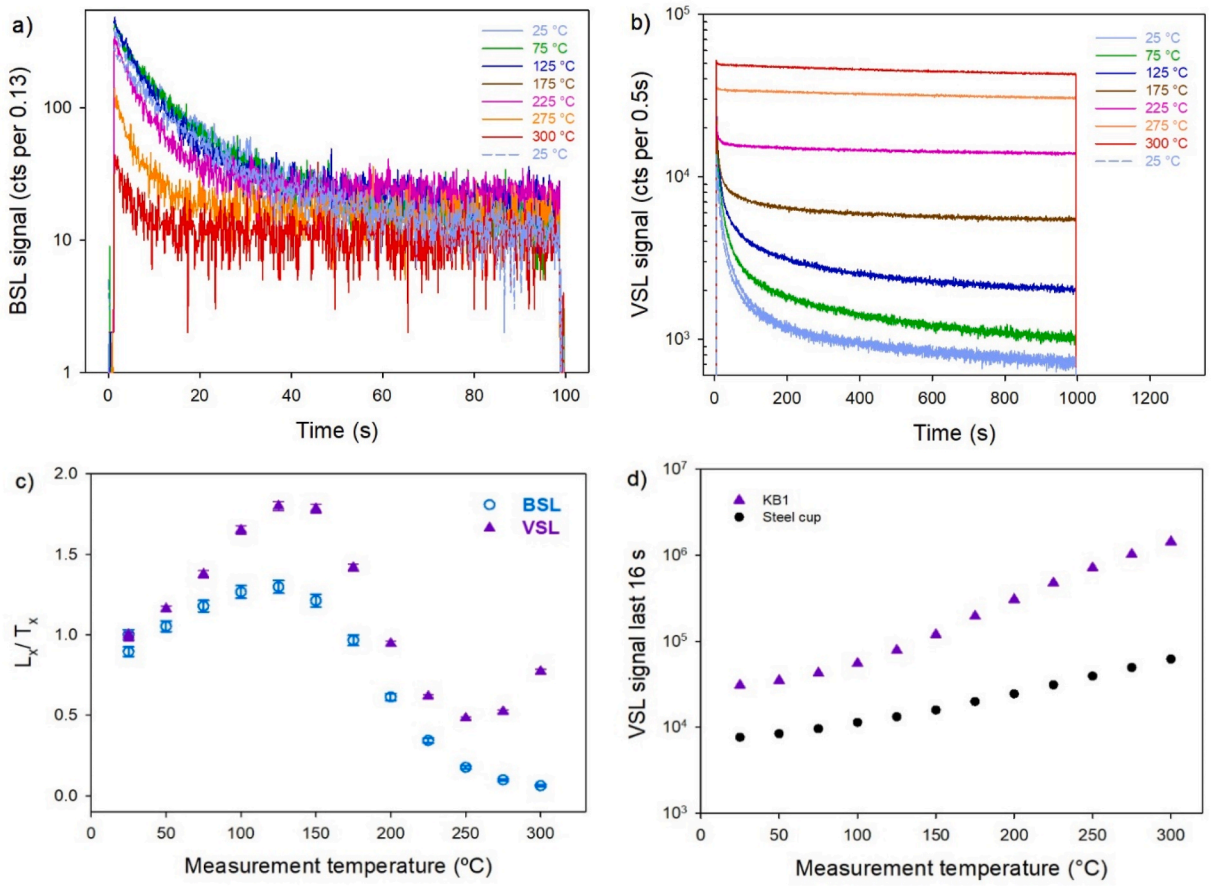

Fig. 3. a) BSL decay curves measured on an annealed aliquot of KB1 at different temperatures. b) Same as a) for VSL decay curves. c) L_x/T_x signal as a function of measurement temperature (initial signal minus a background from the end of each BSL or VSL measurement). L_x/T_x values are normalized to the first measurement point. d) Last 16 s of the VSL signal for sample KB1, and for an empty steel cup versus measurement temperature.

steel cups increases across the range of increasing measurement temperatures, the last 16 s of the VSL measurements from the aliquot of sample KB1 are always higher than those from the steel cup only, and they increase at a faster rate than the background from the empty cup. Two conclusions can be drawn from this observation. First, that even after 1000 s of violet stimulation there is a VSL signal from KB1, and second that there is no indication in these measurements of thermal quenching of this signal. Fig. 3c and d suggest that the VSL signal consists of two parts, one affected by thermal quenching (Fig. 3c) and the other not (Fig. 3d), and from the work of Franklin et al. (1995) we suggest that these two parts (which dominate the early and late part of the VSL signal respectively) are using different recombination centers and originate from different traps. The fact that apparently emissions from both sets of recombination centers are detected through our detection filters is likely due to the breadth of these emissions (see Fig. 1 of Franklin et al., 1995).

The data discussed in Sections 3.1, 3.2 and 3.3 lead us to conclude that a preheat of 340 °C will most effectively separate the VSL signal from the BSL signal, but that even when using this high preheat, the VSL signal consists of two parts. One that is dominant in the earlier part of the VSL decay curve (that shares some of the characteristics of the rapidly bleaching family of Franklin et al., 1995), while the second part likely originates from the 375 °C TL peak and becomes the dominant source of the VSL signal later in the VSL measurement. The next section examines the parameters of a SAR sequence with this information in mind.

4. Optimizing SAR parameters for VSL measurements

Following on from the findings of section 3, the shape of the dose response curve (DRC) for regenerative doses of up to ~8000 Gy using the thermal treatments specified in Table 3 was explored using an aliquot of sample KB1 that had previously been heated to 450 °C. The procedure included VSL measurements lasting 1000 s and a violet bleach at 380 °C for 200 s (higher than the preheat temperature) to attempt to reduce the VSL signal as much as possible prior to the next cycle of measurement. The first 4 s of the VSL signal with late background subtraction (last 16 s) was used. Using a small test dose (~40 Gy), the ratio of L_x/T_x increased for doses from zero to ~1200 Gy (Fig. 4a), but beyond

Table 3
SAR sequence used in this study for dose recovery and D_e measurements. This sequence was also used to build the DRCs in Fig. 4.

Step	Treatment	Purpose	Signal
1	Regenerative Dose		
2	TL at 340 °C for 10 s	Preheat	
3	BSL at 125 °C for 100 s	Remove fast OSL	
4	VSL at 125 °C for 1000 s	Measure VSL	L_x
5*	(VSL at 310 °C for 200 s	Remove VSL)*	
6	Test Dose		
7	TL at 340 °C for 10 s	Preheat	
8	BSL at 125 °C for 100 s	Remove fast OSL	
9	VSL at 125 °C for 1000 s	Measure VSL	T_x
10	VSL at 380 °C for 200 s	Remove VSL	

* Note that the violet bleach shown in step 5 is only used to build the DRC in Fig. 4c.

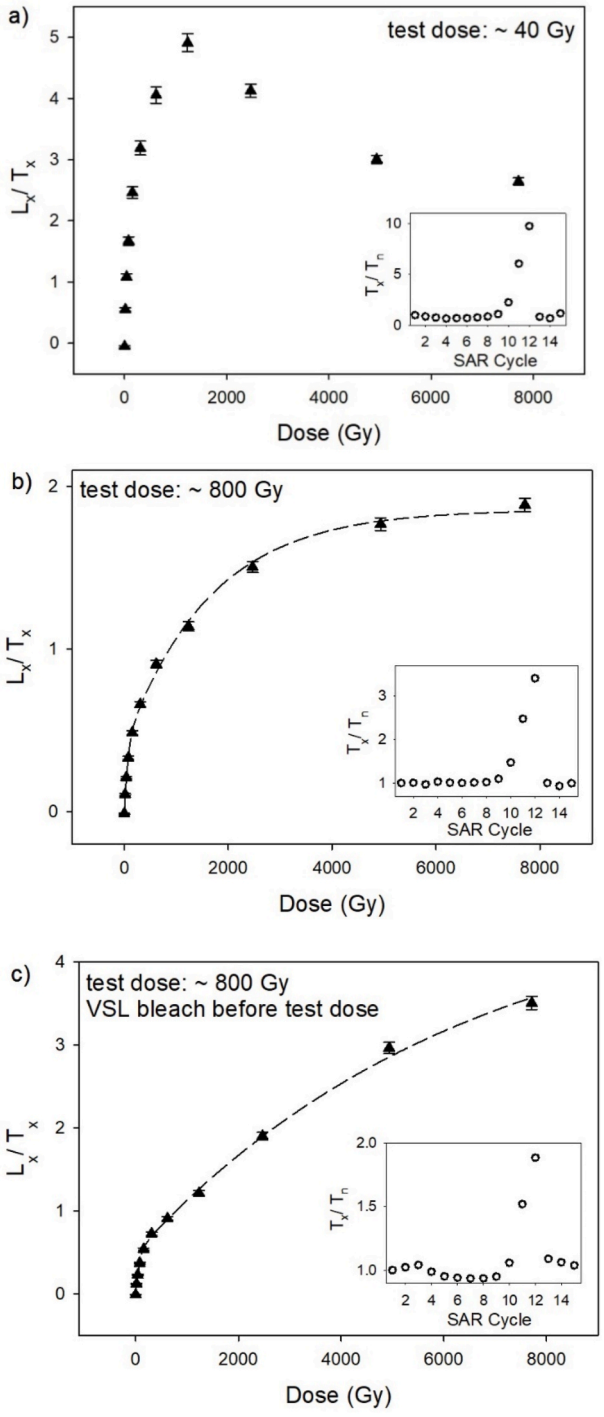

Fig. 4. Dose response curves for an annealed aliquot of quartz from KB1 using the sequence outlined in Table 3 a) Test dose is ~40 Gy. The DRC decreases at doses beyond ~1200 Gy. b) Test dose increased to ~800 Gy. The DRC grows steadily with dose. c) Same test dose as b), but adding a VSL bleach before test dose (step 5 in Table 3). Insets show the sensitivity change. The DRC in b) and c) is fitted by a double exponential function.

this dose the L_x/T_x ratio decreased. Coincident with the decrease in L_x/T_x, a large change in sensitivity is observed, reaching a maximum value of 9.6 for T_x/T_n for the highest regeneration dose of ~8000 Gy (shown in the inset to Fig. 4a). When studying the DRC of feldspars, Colarossi et al. (2018b) saw large changes in sensitivity at low test doses and interpreted this effect as being due to carry over of charge from the regenerative step (L_x measurement) to the test dose step (T_x), and on to the following L_x/T_x cycle, etc; given the difficulty of removing the VSL signal (Fig. 3d) it is possible that a similar process is happening here. One of the solutions of Colarossi et al. (2018b) was to mask this charge carry-over in feldspars using a relatively large test dose compared to the anticipated natural dose, and the same idea was tested in the present VSL study of quartz. Measurements were repeated on the same aliquot, but the test dose was raised from ~40 Gy to ~800 Gy. Unlike Fig. 4a, the resulting DRC (fitted by the sum of two exponentials) grows steadily as the regenerative dose increases up to ~8000 Gy (Fig. 4b). The maximum sensitivity change (T_x/T_n) observed (a value of 3.3) is only about one third of that seen previously with a test dose of 40 Gy, but it is still possible that charge carry over from L_x to T_x exists (Fig. 4b inset). Therefore, the sequence was further modified by implementing a high temperature violet bleach before the test dose (VSL at 310 °C for 200 s; step 5 in Table 3) to reduce the VSL charge carry over from L_x to T_x. With this modification to the SAR protocol, the sensitivity change is reduced again (maximum value for T_x/T_n of 1.8, Fig. 4c inset). The DRC (Fig. 4c) has a similar form to that observed previously (Fig. 4b), requiring the sum of two exponentials for fitting, but the second exponential now has a much larger D_0 value, 5780 ± 633 Gy instead of 1520 ± 102 Gy. D_0 values for the first exponential also increased, but within uncertainties, 67.8 ± 4.8 Gy in Fig. 4c compared with 59.1 ± 5.3 Gy in Fig. 4b.

Separation of the two exponential components in the VSL dose response curve appears to be improved by including the high temperature VSL bleach treatment in step 5 (Table 3), and hence this step was used in dose recovery and D_e evaluations which are described next.

5. Dose recovery

Whilst the examination of dose response curve shape thus far suggests the potential for dating older material using the second exponential component, a key test of any measurement protocol is the ability to recover a known (in this case, laboratory-given) dose. The SAR sequence developed in Section 4 (including the high temperature violet bleach in Step 5 of Table 3) was tested by undertaking a series of dose recovery experiments on sample KB1, using six given laboratory beta doses (0, 15, 100, 400, 1600 and 3200 Gy). Eighteen new aliquots of KB1 that had not received any previous artificial treatment were bleached in the SOL2 solar simulator for 24 h, and split into six groups with three aliquots for each dose to be recovered. The test dose size (Gy) for each set of dose recovery measurements was the same as the given dose, except for the three aliquots used when no laboratory dose was given (0 Gy dose). These three aliquots used a test dose of ~1.5 Gy. The average D_e value measured from the three aliquots which were given zero Gy was subtracted as a residual from all other D_e values before calculating the dose recovery ratio in the following sections.

5.1. Signal integration limits and DRC shape

The effect of selecting different signal and background integration limits upon the shape of the DRC was explored for the data collected from the aliquots receiving a given dose of 400 Gy. For each aliquot and every integration limit, the best fit for the DRC was selected based on the lowest reduced χ^2 value in the Analyst software package; and hence, linear, exponential, exponential plus linear, and sum of two exponential functions were examined in each case.

Fig. 5a shows the decay curve for an aliquot after administering ~400 Gy. Fig. 5b shows the DRC when selecting 0–4 s for the signal integration limits with late background subtraction (last 16 s), which is well-fitted with the sum of two exponential functions, indicating that two separate curves are contributing to the overall shape of this DRC as also seen in Fig. 4c. Using this first part of the signal (0–4 s), the ratio for the recovered to given dose is 1.16, with the recycling ratio just within ±10% of unity (within errors) (Fig. 5b). In contrast, Fig. 5c shows the DRC obtained for the same signal integration limits (0–4 s) but using an early background subtraction (4–20 s) to more effectively isolate the

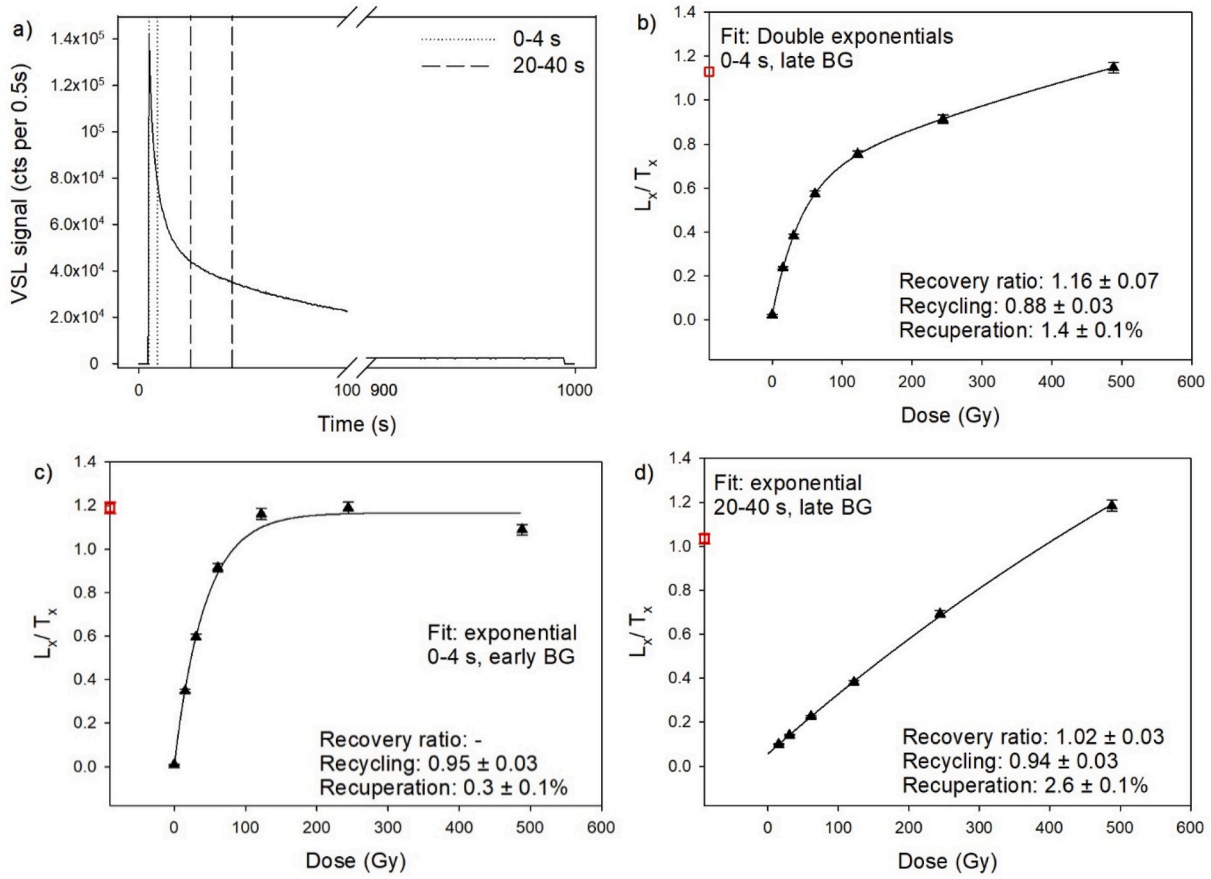

Fig. 5. a) VSL decay curve for the dose recovery experiment after administering ~400 Gy for an aliquot of sample KB1 using the SAR protocol in Table 3. The vertical dotted and dashed lines represent the two signal integration limits selected. b) DRC for the first signal integration limit (0–4 s) using late background (last 16 s). c) Same as b) with early background subtraction (4–20 s) – Signal A. d) DRC for the second signal integration limit (20–40 s) using late background (last 16 s) – Signal B. The red squares on the y axis in b), c), and d) show the L_n/T_n ratio.

rapidly decaying part of the VSL decay curve (Fig. 5a). This is termed Signal A and the DRC obtained with this signal is shown in Fig. 5c. The recycling ratio and recuperation values are improved compared to when the late background subtraction was used (Fig. 5b), and the DRC obtained using Signal A can be fitted by a single saturating exponential function. However, L_x/T_x values do not show any increase for regenerative doses beyond ~120 Gy (Fig. 5c). The L_n/T_n ratio is identical to the maximum signal obtained with regeneration doses, and because the signal is saturated it is not possible to recover the 400 Gy given dose. Moving away from this rapidly decaying part of the VSL signal, different integration limits were tested. While the intensity of this first part of the signal varies between aliquots, the earliest where the characteristics of the DRC changes is 20 s away from the beginning of the decay curve. Therefore, 20–40 s was selected for the signal integration limit. Fig. 5d shows the DRC when the signal from 20 to 40 s is integrated (and a late background is subtracted) to isolate a second VSL signal (Signal B). A clear distinction in the shape and growth of the DRC derived from Signal B is evident compared to that obtained using Signal A (contrast Fig. 5c and d). Using Signal B (Fig. 5d), the given dose is successfully recovered (dose recovery ratio 1.02 ± 0.03) and the recycling ratio is within ±5% of unity (with errors). Using these two (early and later) integration intervals is effective in isolating the two signals of the VSL decay curve and separates the two dose response curve characteristics. The relative intensity of the first VSL signal to the second varies from one aliquot to another, and for some aliquots the DRC based on the first signal is hard to resolve.

5.2. Recovering various doses

Fig. 6 illustrates the dose recovery values obtained for all five recovered doses using Signal A and Signal B identified in Section 5.1. The three aliquots that were bleached in the SOL2 but not given any laboratory dose yielded residual doses of 6.5 ± 3.9 Gy and 5.5 ± 5.5 Gy

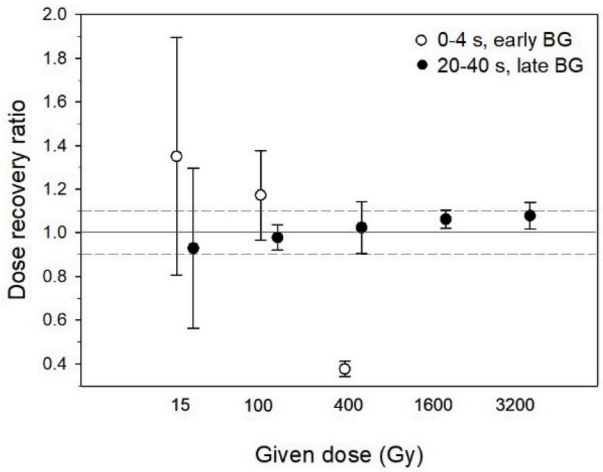

Fig. 6. Dose recovery ratio (i.e. measured dose minus residual dose [Gy], divided by given dose [Gy]) for sample KB1 for various given doses, averaged for three aliquots (two aliquots for 400 Gy with early signal integration).

(for Signal A and Signal B respectively) and these values were subtracted from measured dose values to calculate the dose recovery data shown in Fig. 6. The dose recovery data for the 15 Gy given dose is scattered for both signals, but this is not surprising given that the residual doses are ~30% of the given dose. The early saturation of Signal A (using the early part of the VSL signal (Fig. 5c)) limits dose recovery to doses of ~120 Gy or lower; hence, the 400 Gy given dose is underestimated due to saturation. Moreover, no DRC fit was possible for the higher given doses of 1600 and 3200 Gy. However, the later part of the signal (Signal B; 20–40 s) looks more promising, and all doses were recovered within the 10% range normally used (Fig. 6).

6. D_e determination

For D_e determination, the sequence outlined in Table 3 and tested using the dose recovery experiment in Section 5 was used. The D_e values calculated for samples KB1, KB7, and KB9 in addition to their expected D_e values obtained by single grain quartz BSL and multiple grain quartz TT-OSL are listed in Table 4. Sample KB1 is a young fluvial sample with a single grain quartz BSL D_e of ~1 Gy (Table 4). The calculated D_e values based on Signal A and Signal B (17.3 ± 6.7 Gy for 0–4 s, 26.7 ± 10.6 Gy for 20–40 s; Table 4) overestimate the expected D_e. This is similar to the findings of Ankjærgaard et al. (2013) who observed significant overestimation (by ~180%) of the expected D_e for their youngest sample regardless of the VSL component selected (their component A or B). KB1 exhibits considerable overdispersion (74%) in single grain quartz BSL D_e values and the minimum age model was used to derive a final D_e (Duller et al., 2015); since the VSL signal bleaches more slowly than the BSL, the high VSL D_e values are not surprising. On the other hand, comparison of our calculated VSL D_e values with the TT-OSL D_e for this sample (102 ± 10 Gy, Duller et al., 2015) reveals that the quartz VSL signal appears to be better bleached in nature than the TT-OSL signal.

For sample KB9, the use of Signal A resulted in a D_e (119 ± 43 Gy) that overestimated the expected D_e by almost a factor two (Table 4), and it is not clear why this should be the case, though the large uncertainty in the D_e is notable. In contrast, the D_e calculated using Signal B (51 ± 5 Gy) is much closer to the expected D_e (62.5 ± 1.6 Gy; Table 4).

Sample KB7 has an expected D_e value of 511 ± 22 Gy based on TT-OSL (Duller et al., 2015). Fig. 7a shows the natural and a regenerative dose VSL decay curve for this sample and the corresponding DRCs for this aliquot are shown in Fig. 7b and c. As expected from the dose recovery experiment, the use of Signal A resulted in a saturated DRC (Fig. 7b) and hence is not suitable for D_e evaluation beyond the limit of conventional quartz OSL dating. Using Signal B produced a DRC that continues to grow with dose (Fig. 7c), very like that seen for KB1 (Fig. 5d); however, the D_e value is only ~8% of the expected D_e value. Since Signal B was successful in recovering different given doses (Fig. 6), this underestimation in D_e is not due to saturation but could be explained by thermal instability of this signal over geological time.

Table 4
Equivalent dose (D_e) values for three samples from Zambia. 'n' indicates the number of aliquots used for D_e calculation. Recycling is within uncertainties of unity in all cases. Recuperation as percent of natural is shown in each case.

Sample	Test dose (Gy)	Signal A: (0–4s)			Signal B: (20–40s)			Expected D_e (Gy)
		n	De (Gy)	Recup (% nat)	n	De (Gy)	Recup (% nat)	Duller et al. (2015)
KB1	3.8	6	17.3 ± 6.7	≤5.2	4	26.7 ± 10.6	≤40.3	1.34 ± 0.05[a]
KB9	37.5	6	119 ± 43	0	6	51 ± 5	≤2.1	62.5 ± 1.6[b]
KB7	75	3	100 ± 27	≤0.2	6	40 ± 8	≤4.5	511 ± 22[c]

Notes.
In each case, six aliquots were measured. For KB1 when using Signal B, two aliquots with negative D_e values were not included. For KB7 when using Signal A, three aliquots fail to provide D_e due to saturation.
Expected D_e values were calculated by Duller et al. (2015) using different methods.
[a] Single grain quartz OSL using the minimum age model.
[b] single grain quartz OSL using central age model.
[c] multiple grain thermally-transferred OSL (TT-OSL) using the central age model. The residual subtracted TT-OSL D_e is 400 ± 23 Gy.

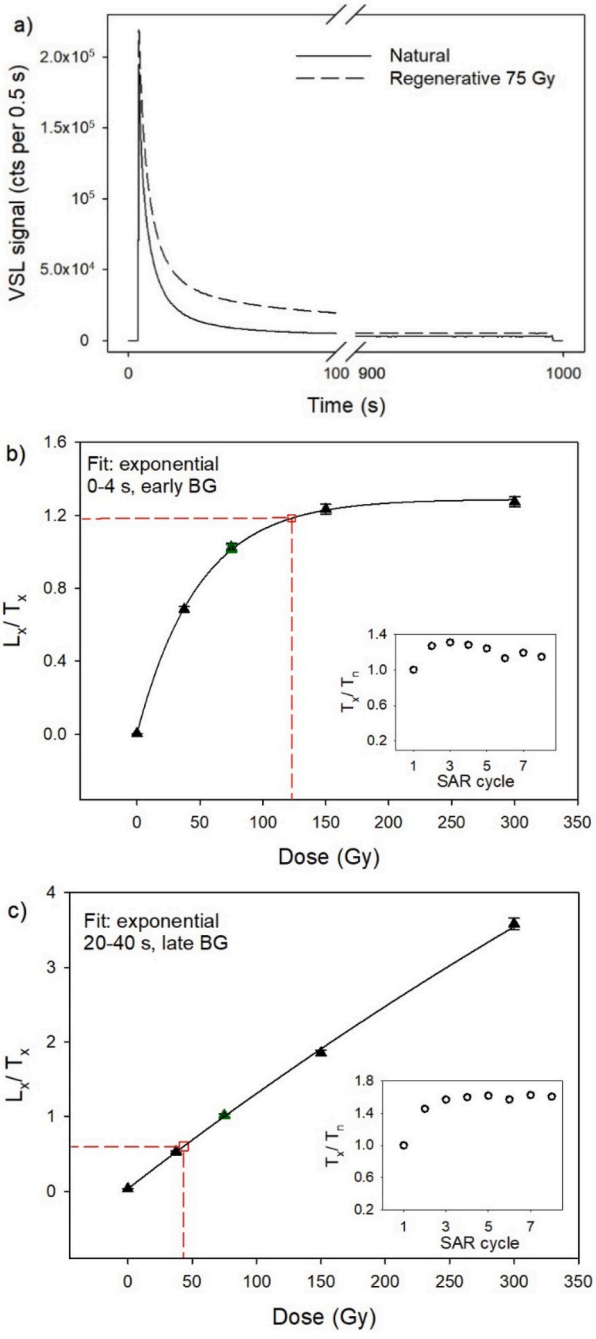

Fig. 7. a) Natural and regenerative decay curves for one aliquot of sample KB7. b) The DRC for that aliquot for 0–4 s of the signal – Signal A. c) Same as b) for 20–40 s of the signal – Signal B. In both b) and c) the DRC fit is exponential. The green open triangles show the recycled point and the interpolation of the L_n/T_n to the DRCs is shown by red squares. Insets in b) and c) show sensitivity change.

Analysis in Section 3.3 concluded that Signal B was associated with the 375 °C TL peak, consistent with previous work by Ankjærgaard et al. (2013) and Hernandez and Mercier (2015). The lifetime of the 375 °C TL peak is poorly constrained, with Fleming (1979) giving a value of $\geq 10^8$ years at 15 °C, but this would imply that stability ought not to be a problem for the time period we are dating at Kalambo Falls. Furthermore, Ankjærgaard et al. (2013, 2015) and Rahimzadeh et al. (2021) reported thermal stability for the VSL signal of $\sim 10^{11}$ years at 10 °C, again implying that stability should not be a limiting factor. We are therefore left in the situation that kinetic studies suggest the VSL Signal B should be stable over the time periods we are trying to date, but our measurements of D_e (Table 4) are most easily explained by the signal being unstable over geological time.

7. Summary and conclusions

One of the main reasons for selecting the VSL signal for dating is the observation that it saturates at much higher doses in the laboratory compared to the conventional BSL signal for quartz. However, it is evident from the literature that the D_e values based on the VSL signal (by either single or even in some cases multiple aliquot methods) have been in agreement with independent age controls when testing younger samples (<~200 Gy; Ankjærgaard et al., 2016; Porat et al., 2018) and underestimated the expected D_e when considering older samples (>~200 Gy; Ankjærgaard et al., 2015, 2016; Morthekai et al., 2015; Colarossi et al., 2018a; Sontag-González et al., 2021; Rahimzadeh et al., 2021). In this study, and in order to investigate the origins of the VSL signal from quartz, the behavior of this signal with respect to thermal treatments was investigated. Results from these experiments suggest that the VSL signal is derived from two families of traps in quartz; a group that demonstrate thermal quenching and has small D_0 values (<100 Gy) (this group may be associated with the 'rapidly bleaching family' of Franklin et al., 1995), and another group that does not suffer from thermal quenching and has high D_0 values (probably related to the 'slowly bleaching family' of Franklin et al., 1995, namely the 375 °C TL peak). The distinct DRC behavior seen from the two parts of the VSL signal (Fig. 5c and d) may be linked to these separate source traps giving rise to this signal.

A VSL SAR protocol was subsequently modified from previous research based on the results of pulse annealing and DRC growth behavior for one of our three samples. The suitability of this newly developed SAR protocol was then further tested by conducting a series of dose recovery experiments. Successful recovery ratios were obtained when the first rapidly decaying part of the signal was avoided, and consequently, two signal and background integration limits were considered. The DRC is best fitted with the sum of two exponential functions when considering the first part of the decay curve (with late background subtraction) in all of the experiments (sections 4, 5 and 6) which seems to be indicating a mixture of the two signals in the VSL decay curve. However, if isolating Signal A, the DRC fit becomes exponential (see Figs. 5c and 7b) with a small D_0 value; while selecting Signal B, the DRC fit also becomes exponential but with a large D_0 value and the potential to grow to high doses (see Figs. 5d and 7c). Ankjærgaard et al. (2013) also examined two different integration limits, termed components A and B and representing the early faster decaying part of the signal and the later slower decaying signal, respectively. Although Ankjærgaard et al. (2013) found larger D_e values when using their component A, Sontag-González et al. (2021) found larger D_e values with component B of Ankjærgaard et al. (2013). In the present study, in spite of obtaining larger D_e values for the two older samples (KB7 and KB9) when using the early part of the signal, similar to findings of Ankjærgaard et al. (2013), the DRC becomes close to saturation at ~150 Gy and hence the D_e values have large uncertainties (~30% of the calculated D_e, see samples KB9 and KB7 in Table 4). In contrast, the DRC derived from the later slower decaying part of the signal grows to high doses in the laboratory and is fitted by an exponential function with only slight curvature at doses up to ~500 Gy (see Figs. 5d and 7c). However, the calculated D_e value for our oldest sample (KB7) based on this slower decaying part of the signal underestimates the expected D_e value significantly. Considering the successful laboratory dose recovery results obtained using late integration of the VSL signal, such underestimation of the natural D_e may suggest instability of this signal over time for our samples.

Declaration of competing interest

The authors declare that they have no known competing financial interests or personal relationships that could have appeared to influence the work reported in this paper.

Acknowledgements

This research was conducted while NA was undertaking a PhD funded by an AberDoc Scholarship and a President's Scholarship awarded by Aberystwyth University. We are grateful to an anonymous reviewer and Alicja Chruscinska for their constructive comments which improved the paper.

References

Ankjærgaard, C., 2019. Exploring multiple-aliquot methods for quartz violet stimulated luminescence dating. Quat. Geochronol. 51, 99–109.
Ankjærgaard, C., Guralnik, B., Buylaert, J.-P., Reimann, T., Yi, S., Wallinga, J., 2016. Violet stimulated luminescence dating of quartz from Luochuan (Chinese loess plateau): agreement with independent chronology up tō 600 ka. Quat. Geochronol. 34, 33–46.
Ankjærgaard, C., Guralnik, B., Porat, N., Heimann, A., Jain, M., Wallinga, J., 2015. Violet stimulated luminescence: geo-or thermochronometer? Radiat. Meas. 81, 78–84.
Ankjærgaard, C., Jain, M., Wallinga, J., 2013. Towards dating Quaternary sediments using the quartz Violet Stimulated Luminescence (VSL) signal. Quat. Geochronol. 18, 99–109.
Barham, L., Tooth, S., Duller, G.A.T., Plater, A.J., Turner, S., 2015. Excavations at site C north, Kalambo Falls, Zambia: new insights into the mode 2/3 transition in south-central Africa. J. Afr. Archaeol. 13, 187–214.
Colarossi, D., Chapot, M.S., Duller, G.A.T., Roberts, H.M., 2018a. Testing single aliquot regenerative dose (SAR) protocols for violet stimulated luminescence. Radiat. Meas. 120, 104–109.
Colarossi, D., Duller, G.A.T., Roberts, H.M., 2018b. Exploring the behaviour of luminescence signals from feldspars: implications for the single aliquot regenerative dose protocol. Radiat. Meas. 109, 35–44.
Duller, G.A.T., Tooth, S., Barham, L., Tsukamoto, S., 2015. New investigations at Kalambo Falls, Zambia: luminescence chronology, site formation, and archaeological significance. J. Hum. Evol. 85, 111–125.
Faershtein, G., Porat, N., Matmon, A., 2020. Extended range luminescence dating of quartz and alkali-feldspar from aeolian sediments in the eastern Mediterranean. Geochronl. Discuss. 1–36, 2020.
Fleming, S.J., 1979. Thermoluminescence Techniques in Archaeology. Clarendon Press, Oxford.
Franklin, A.D., Prescott, J.R., Scholefield, R.B., 1995. The mechanism of thermoluminescence in an Australian sedimentary quartz. J. Lumin. 63, 317–326.
Hernandez, M., Mercier, N., 2015. Characteristics of the post-blue VSL signal from sedimentary quartz. Radiat. Meas. 78, 1–8.
Jain, M., 2009. Extending the dose range: probing deep traps in quartz with 3.06 eV photons. Radiat. Meas. 44, 445–452.
Jain, M., Murray, A.S., Bøtter-Jensen, L., 2003. Characterisation of blue-light stimulated luminescence components in different quartz samples: implications for dose measurement. Radiat. Meas. 37, 441–449.
Lapp, T., Jain, M., Thomsen, K.J., Murray, A.S., Buylaert, J.-P., 2012. New luminescence measurement facilities in retrospective dosimetry. Radiat. Meas. 47, 803–808.
Lapp, T., Kook, M., Murray, A.S., Thomsen, K.J., Buylaert, J.P., Jain, M., 2015. A new luminescence detection and stimulation head for the Risø TL/OSL reader. Radiat. Meas. 81, 178–184.
Morthekai, P., Chauhan, P.R., Jain, M., Shukla, A.D., Rajapara, H.M., Krishnan, K., Sant, D.A., Patnaik, R., Reddy, D.V., Singhvi, A.K., 2015. Thermally re-distributed IRSL (RD-IRSL): a new possibility of dating sediments near B/M boundary. Quat. Geochronol. 30, 154–160.
Murray, A.S., Wintle, A.G., 2000. Luminescence dating of quartz using an improved single-aliquot regenerative-dose protocol. Radiat. Meas. 32, 57–73.
Porat, N., Jain, M., Ronen, A., Horwitz, L.K., 2018. A contribution to late middle paleolithic chronology of the levant: new luminescence ages for the atlit railway bridge site, coastal plain, Israel. Quat. Int. 464, 32–42.
Rahimzadeh, N., Tsukamoto, S., Zhang, J., Long, H., 2021. Natural and laboratory dose response curves of quartz violet stimulated luminescence (VSL): exploring the multiple aliquot regenerative dose (MAR) protocol. Quat. Geochronol. 65, 101194.

Roberts, H.M., Duller, G.A.T., 2004. Standardised growth curves for optical dating of sediment using multiple-grain aliquots. Radiat. Meas. 38, 241–252.
Singarayer, J., Bailey, R., 2003. Further investigations of the quartz optically stimulated luminescence components using linear modulation. Radiat. Meas. 37, 451–458.
Sontag-González, M., Frouin, M., Li, B., Schwenninger, J.-L., 2021. Assessing the dating potential of violet stimulated luminescence protocols. Geochronometria 48, 121–128.
Spooner, N.A., 1994. On the optical dating signal from quartz. Radiat. Meas. 23, 593–600.
Wintle, A.G., 1975. Thermal quenching of thermoluminescence in quartz. Geophys. J. Int. 41, 107–113.